AJNR

Improved Microsurgical Creation of Venous Pouch Arterial Bifurcation Aneurysms in Rabbits

C. Sherif, S. Marbacher, S. Erhardt and J. Fandino

AJNR Am J Neuroradiol 2011, 32 (1) 165-169
doi: https://doi.org/10.3174/ajnr.A2235
http://www.ajnr.org/content/32/1/165

ORIGINAL RESEARCH

C. Sherif
S. Marbacher
S. Erhardt
J. Fandino

Improved Microsurgical Creation of Venous Pouch Arterial Bifurcation Aneurysms in Rabbits

BACKGROUND AND PURPOSE: The choice of the experimental aneurysm model is essential for valid embolization-device evaluations. So far, the use of the rabbit venous pouch arterial bifurcation aneurysm model has been limited by demanding microsurgery, low aneurysm patency rates, and high mortality. This study aimed to facilitate microsurgery and to reduce mortality by optimized peri-/postoperative management.

MATERIALS AND METHODS: Aneurysms were created in 16 New Zealand white rabbits under general intravenous anesthesia. Using modified microsurgical techniques, we sutured a jugular vein pouch into a bifurcation created between both CCAs. Aggressive anticoagulation (intraoperative intravenous: 1000-IU heparin, 10-mg acetylsalicylic acid/kg; postoperative subcutaneous: 14 days, 250-IU/kg /day heparin) and prolonged postoperative anesthesia (fentanyl patches: 12.5 μg/h for 72 hours) were applied. Angiographic characteristics of created experimental aneurysms were assessed.

RESULTS: The reduced number of interrupted sutures and aggressive anticoagulation caused no intra-/postoperative bleeding, resulting in 0% mortality. Four weeks postoperation, angiography showed patency in 14 of 16 aneurysms (87.5%) and Ohshima type B bifurcation geometry. Mean values of parent-artery diameters (2.3 mm), aneurysm lengths (7.9 mm), and neck widths (4.1 mm) resulted in a mean 1.9 aspect ratio.

CONCLUSIONS: Compared with historical controls, the use of modified microsurgical techniques, aggressive anticoagulation, and anesthesia resulted in higher aneurysm patency rates and lower mortality rates in the venous pouch arterial bifurcation aneurysm model. Gross morphologic features of these aneurysms were similar to those of most human intracranial aneurysms.

ABBREVIATIONS: CCA = common carotid artery; DSA = digital subtraction angiography

Endovascular embolization of intracranial aneurysms has become an equivalent alternative to clipping for ruptured aneurysms, especially in regard to short-term results.[1] However, disappointing long-term results with unacceptably high rates of aneurysm recanalization and late aneurysm re-rupture were shown recently in large clinical trials.[2] Thus, experimental animal studies are crucial to test new and better endovascular devices, to improve long-term aneurysm occlusion.[3-5]

The choice of the model is essential for the comparability of experimental findings with human conditions.[6] In a comparison of the currently used animal models in rats, rabbits, canines, and swine,[7-9] the rabbit model showed advantageous comparability with the human coagulation system and the best cost-effectiveness.[10-12]

At the moment, the most frequently used aneurysm model is the rabbit elastase model,[13-15] based on intraluminal perfusion of the stump of 1 CCA with pancreatic elastase. The main advantages of this model are the relatively easy microsurgical technique, high aneurysm patency, and low morbidity.[12,16,17] However, the aneurysm wall of elastase aneurysms consists of a former elastic artery, the multiple elastic membranes of which were destructed by elastase, probably causing a long-lasting inflammatory repair process in the entire aneurysm wall.[18] Additionally, approximately 65%–85% of ruptured human intracranial aneurysms arise directly at bifurcations.[19] However, elastase aneurysms are sidewall aneurysms that continue into an altered wall of a branching artery, as can be seen on 3T MR angiographic images.[20] In particular his lack of true bifurcational hemodynamics seems to be the major drawback of this model.[21]

In general, arterial sidewall aneurysm models cannot predict the ability of new coils to improve long-term angiographic results under more challenging hemodynamic conditions.[6] For example, it was shown by computer-assisted morphometric comparison of various aneurysm models that bare platinum coils performed equally as well as HydroCoils (MicroVention Terumo, Aliso Viejo, California) only in a canine arterial sidewall aneurysm model, while in arterial bifurcation models, HydroCoils provided better long-term stable occlusion.[18]

In contrast, the venous pouch arterial bifurcation model is created by a venous pouch sutured into an artificial true bifurcation of both CCAs. The postulated main advantages of this model are true bifurcational hemodynamics[21] and the possibility of varying the anatomy of the bifurcation and neck/fundus size of the aneurysm.[6] The postulated histomorphologic drawback is a supposed pronounced foreign body reaction around the suture lines at the neck plane, impairing thrombus organization and fibrovascular healing.[10] However, it has already been shown that the foreign body response to the monofilament sutures around the anastomosis is only benign and

Received February 23, 2010; accepted after revision June 6.

From the Department of Neurosurgery (C.S., S.M., J.F.), Cantonal Hospital of Aarau, Switzerland; and Departments of Intensive Care Medicine (C.S., S.M., S.E., J.F.) and Neurosurgery (J.F.), Cerebrovascular Research Group, University Hospital Berne, Berne, Switzerland.

This work was supported by Boston Scientific Inc, who provided their technical support; S&T Microsurgical Instruments Inc, who provided us the microsurgical equipment; and Ethicon Inc, who provided the suture material.

Please address correspondence to Camillo Sherif, MD, Department of Neurosurgery, Cantonal Hospital of Aarau, Tellstr, CH-5000, Switzerland; e-mail: camillo.sherif@ksa.ch

DOI 10.3174/ajnr.A2235

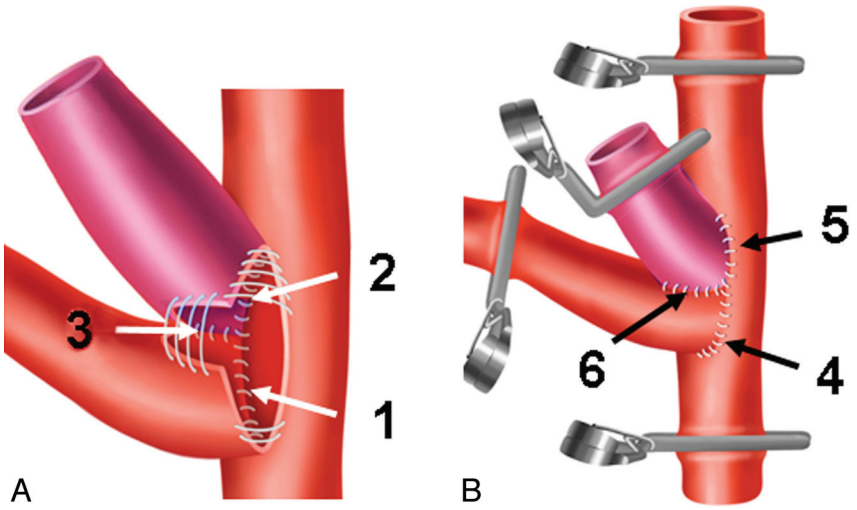

Fig 1. Microsurgical steps during venous pouch arterial bifurcation aneurysm creation. *A,* Suturing sequence at the posterior aspect of the anastomosis: 1) right to left CCA, 2) venous pouch to left CCA, 3) venous pouch to right CCA. *B,* Suturing sequence at the anterior aspect: 4) right to left CCA, 5) venous pouch to left CCA, 6) venous pouch to right CCA.

that this chronic inflammatory reaction to nonresorbable sutures is locally confined to the outer parts of the respective vessel walls.[5,22] What is more, the aneurysm wall in the venous pouch arterial bifurcation model consists of an unaltered vein transplant with just a few elastic membranes. These features can also be seen in human intracranial aneurysm walls.[23] The major shortcomings, resulting in less frequent use of this aneurysm model in recent years, are the high demands of the microsurgical technique, low aneurysm patency rates, and high morbidity rates ≤50%.[6,24]

The present study aimed to show that these shortcomings could be minimized by facilitating microsurgical procedures and improved peri-/postoperative management.

Materials and Methods

The aneurysms were created in 16 female New Zealand white rabbits (body weight, 3.1–4.7 kg). All surgical procedures were performed at the Department of Clinical Research at the University of Berne. The study was approved by the responsible veterinarian agency of the Canton of Berne, Switzerland.

Anesthesia

All rabbits were premedicated with subcutaneous injection of 65-mg/kg xylazine and 4-mg/kg ketamine and received, preoperatively, a single dose of antibiotics (50-mg penicillin) intravenously. For general anesthesia, a solution of 130-mg/kg xylazine and 8-mg/kg ketamine in 100-mL 0.9% saline was intravenously administered via a perfusor with a rate of 1 mL/s. Animals received oxygen (1 L/min) via ventilation mask.

Microsurgical Aneurysm Creation

The animals were fixed in a supine position on a body warming plate. All operative procedures were performed under sterile conditions. A midline incision was made from the manubrium sterni up to the jaw. The following microsurgical procedures were performed by using an operation microscope: First, a 1.5-cm-long segment of the left external jugular vein without venous branches was prepared, ligated proximally and distally with 4–0 silk (Ethilon 4–0; Ethicon, West Somerville, New Jersey), resected, and kept in heparinized saline (a mixture of 1000-IU heparin in 20-mL 0.9% saline and 1-mL papaverin HCl 4%). The left CCA was then prepared over a distance of approximately 5 cm, starting from the aortic arch to the carotid bifurcation. Tiny arterial branches running medially and supplying laryngeal and tracheal structures and neural structures were preserved. The right CCA was then also isolated and mobilized up to the carotid bifurcation and proximally down to the brachiocephalic branching. Then the animals received 1000-IU heparin intravenously. To obtain a long donor artery for a tensionless anastomosis, we temporarily clipped the right CCA distally just below the carotid bifurcation and then proximally ligated it above the brachiocephalic branching and cut it just above this ligature. This stump was extensively irrigated with heparinized saline as described above, and the adventitia at the cut free end was carefully resected.

The segment of the left CCA planned for the anastomosis was also meticulously freed of the adventitia and then temporarily clipped distally and proximally. Between the clips, an elliptic arteriotomy was performed to accommodate the circumferences of the right CCA and the venous pouch, and then this portion between the clips was also extensively irrigated with heparinized saline to remove intraluminal clots. The posterior circumference of the right CCA stump was now sutured into the arteriotomy in the left CCA, by using 4–5 nonresorbable monofilament sutures (Ethilon10–0; Ethicon). Then a longitudinal cut was made in the stump of the right CCA to accommodate half the circumference of the venous pouch. The back side of the venous pouch wall was now first anastomosed with the arteriotomy in the left CCA by again using 4–5 sutures, and then it was anastomosed with the cut in the right CCA with 3–4 sutures (Fig 1*A*). The same procedures were performed in the same order at the anterior side of the anastomosis (Fig 1*B*). Then the distal end of the venous pouch was clipped, and the distal clips on the right CCA were removed. After prompt filling of the aneurysm, trapped air and debris were washed out by opening the clip at the dome of the venous pouch, which was then tightly sealed with a 4–0 polyfilament suture (Vicryl, Ethicon). The suture lines around the anastomosis and the aneurysm neck were then covered with small pieces of adipose tissue for additional hemostasis (Fig 2*A*). During the operation, 4% papaverin HCl solution and antibiotic solution (neomycin sulfate, 5 mg/mL) was frequently ap-

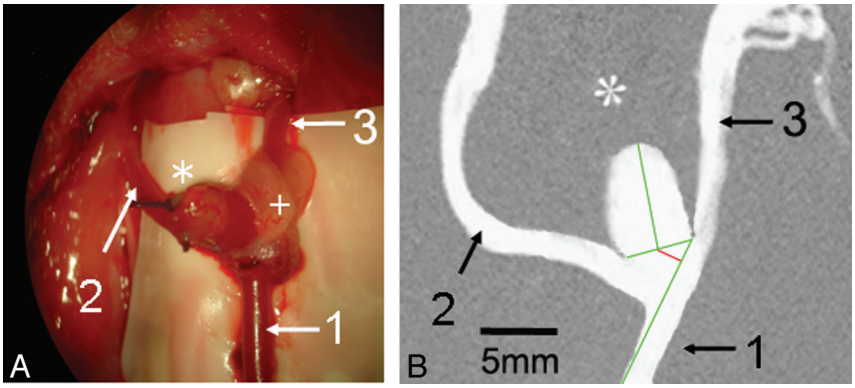

Fig 2. Morphology of the venous pouch arterial bifurcation aneurysm. *A*, View under the operation microscope after microsurgery. *B*, Calibrated DSA 4 weeks after operation. *A*, 1) Proximal left CCA, 2) right CCA, 3) distal left CCA. Asterisk indicates the dome of the venous pouch aneurysm; the plus sign, the fat pad for sealing the suture line. *B*, DSA shows the aneurysm and parent-vessel patency after 4 weeks. Green lines indicate the aneurysm neck width and aneurysm length and the contour of the in-flow parent-artery (left CCA). Red line shows the distance of the neck plane center from the parent-artery contour.

plied topically on the anastomoses to prevent vasospasm and local infections.

For deep and superficial wound closure, 4–0 resorbable sutures (Monocryl, Ethicon) were used.

Postoperative Management

Immediately after we finished the operation, all animals received 10-mg/kg acetylsalicylic acid intravenously and 60-mL 5% glucose subcutaneously to compensate for dehydration during surgery. For prolonged anesthesia, transdermal fentanyl matrix patches releasing 12.5 μg/h were applied for 72 hours in the shaved neck region of the animals. All animals received daily 250-IU/kg low-molecular heparin subcutaneously for 2 weeks.

Angiographic Follow-Up

Four weeks postoperatively, all animals underwent DSA, performed with the animal under general anesthesia, by using standard techniques via a transfemoral approach.[21] To assess the gross morphologic characteristics, we measured the aneurysm parameters, total length, neck width, and parent-vessel diameters (at the level of the aneurysm orifice) on DSA images and calibrated them by paravertebrally placed skin clamps. The aneurysm aspect ratio (length/neck width) was calculated.[25] Additionally, the distance of the neck plane center from the contour of the parent artery was measured (Fig 2*B*) to determine the Ohshima-type bifurcation aneurysm.[26]

All animals showing a patent aneurysm at follow-up were not killed but were included in ongoing experiments at the Department of Clinical Research of the University of Berne.

Results

With the modified microsurgery, on average, 150 minutes were needed for the operations, decreasing from 225 to 115 minutes in the course of the experimental series. The duration of the clamping time of both CCAs was, on average, 65 minutes, decreasing from approximately 120 to 45 minutes. Altogether, on average, 22 interrupted sutures (range, 20–29) were needed to create the anastomoses and aneurysms.

Perioperative and postoperative mortality was 0%. Despite intra- and postoperative high-dose heparinization, no spontaneous bleeding occurred at the site of the anastomoses. No postoperative wound infections and no gastric stress ulcera were observed in the present series; however, 1 animal (the heaviest at 4.7 kg) was impaired by slight hemiparesis but survived until follow-up.

Angiographic Follow-Up

Four weeks postoperatively, DSA showed patency of both CCAs and the aneurysms in 14 of 16 animals (87.5%), while aneurysm occlusion was observed in the hemiparetic animal (4.7 kg) and another animal (4.5 kg). Both aneurysms were created, however, at the beginning of the series (aneurysms 1 and 8). As measured on the calibrated DSAs, parent-artery diameters ranged between 1.6 and 2.7 mm (mean, 2.3 mm), the mean aneurysm length was 7.9 mm (range, 7.4.–8.6 mm), and the mean aneurysm neck width was 4.1 mm (range, 3.7–4.8 mm). These measurements resulted in a mean aspect ratio of 1.9 (range, 1.67–2.08). The neck orifice positioning in relation to the parent-artery axis (Fig 2*B*) showed a mean distance of 1.7 mm (range, 1.3-2.1 mm), thus corresponding to Ohshima type B aneurysms (Table). In human aneurysms, this type B geometry is statistically significantly correlated with a high risk of aneurysm rupture.[26]

Discussion

The results of the present study favor the venous pouch arterial bifurcation aneurysm model in rabbits. Unfortunately, in the available literature on this model, only general descriptions of the operative technique can be found, without special emphasis on surgical details or the importance of peri- and postoperative management strategies.[4,21,24,27] In the authors' opinion, the following factors play key roles in facilitating microsurgery and improving the outcome of this experimental aneurysm creation:

1) Careful preparation of a long segment of the left CCA, but without destruction of the superior laryngeal nerves and small vessels.

2) Careful removal of the highly thrombogenic adventitial connective and fatty tissue from both parent arteries at the planned junction before the creation of the anastomosis.

3) Creation of a tensionless anastomosis between both CCAs. Apparently, it makes no difference that in the present series, the right CCA was anastomosed to the left CCA, in contrast to the originally described and later modified procedure.[21]

Angiographic evaluation							
Aneurysm No.	Patency	Parent Artery ø (mm)	Length (mm)	Neck Width (mm)	Aspect Ratio	Ohshima Shift (mm)	Ohshima Type
1	No						
2	Yes	2.40	8.40	4.70	1.79	1.60	B
3	Yes	1.90	7.70	3.70	2.08	1.70	B
4	Yes	2.60	7.50	3.90	1.92	1.80	B
5	Yes	2.70	7.50	4.10	1.83	1.60	B
6	Yes	2.50	8.00	4.20	1.90	2.10	B
7	Yes	1.90	8.60	4.30	2.00	1.80	B
8	No						
9	Yes	2.60	8.00	4.00	2.00	2.10	B
10	Yes	2.40	8.10	4.10	1.98	1.50	B
11	Yes	1.90	7.60	3.90	1.95	1.30	B
12	Yes	1.60	7.40	3.80	1.95	1.40	B
13	Yes	1.90	7.40	4.10	1.80	2.10	B
14	Yes	2.40	7.10	4.10	1.73	1.80	B
15	Yes	2.30	7.90	4.20	1.88	1.50	B
16	Yes	2.50	8.00	4.80	1.67	2.00	B

4) Reduction of the number of sutures and adjustment of the sequence of suturing around the anastomosis. The number of necessary sutures could be reduced to an average of 22, compared with the ≥32 sutures reported in the literature.[21,24] For the sequence of suturing, the proposed beginning at the posterior aspect of the anastomosis (Fig 1) gives better visual control of these most difficult sutures, in contrast to previously proposed procedures.[21,24,27]

5) The intimal layer around the anastomosis may not be penetrated by sutures, to avoid intimal damage causing thrombosis in the parent arteries. A reduced number of sutures also causes less injury to the vessel walls, further minimizing the risk of aneurysm thrombosis or embolism.

6) Sealing of the outside of the suture lines with a thin layer of fatty tissue proved important to avoid bleeding from the anastomoses, despite the reduced number of sutures and the aggressive anticoagulation regimen, as discussed below.

7) A reduced number of sutures results in shorter clamping times of both CCAs and shorter operation times, reducing the risk of neurologic deficits and complications from anesthesia.

Improved Anticoagulation Management

With the prolonged and more aggressive anticoagulation regimen, a high 87.5% aneurysm and parent-vessel patency could be achieved, but without the incidence of spontaneous aneurysm hemorrhage. These findings go along with Grunwald et al,[28] who showed that combined anticoagulation provides good long-term parent-vessel patency.

Improved Peri- and Postoperative Management

In our opinion, a main factor in reducing the reported high rates of ≤26.3% postoperative respiratory complications[21] was to replace intubation ventilation with general intravenous anesthesia. With the applied intravenous medication, combined with oxygen mask ventilation, satisfactory general anesthesia over the long operation time could be achieved. Furthermore, preservation of the superior laryngeal nerves during careful microsurgical dissection is also crucial for good respiratory outcomes. With this management, we did not observe any respiratory complications in the present series.

Other frequently reported postoperative complications are gastrointestinal problems, mainly caused by stress ulcera, reaching an incidence of ≤20%.[21] Consequently, in the present series, we tried to provide intensified long-term anesthesia for 72 hours, compared with the standard of 24 hours. Obviously, this high dose and extended anesthesia reduced procedural stress for the animals considerably, evidenced by lack of complications with the postoperative nutrition in this series.

The only animal with postoperative hemiparesis was the heaviest animal in this series (4.7 kg) with an extensive subcutaneous fat layer. The second animal showing aneurysm occlusion also had a high body weight of 4.5 kg. Thus, it can be suspected that comparable with human patients, operative risks are higher for overweight subjects. For future experimental series, we suggest using only rabbits with <3.5 kg body weight.

The applied modifications of microsurgery and management resulted in 0% peri-/postoperative mortality in the present study. Thus the major limitation of this aneurysm model[6] was apparently overcome. Despite the small number of animals who underwent surgery, this favorable mortality rate is comparable with the 8.4% mortality reported by Lewis et al[29] during elastase aneurysm creation in an extremely large series of 700 rabbits undergoing surgery. The aneurysm patency rate of 87.5% in the present study is comparable with the 90%–95% patency rates reported for the elastase model.[17,30,31] Because both occluded aneurysms were created in the beginning of the series, this result can be attributed to the surgical learning curve. Thus, it is likely that increasing patency rates can be obtained in larger series of the venous pouch model, achieving the level documented for the elastase model.[29]

Conclusions

The improved venous pouch arterial bifurcation aneurysm model using modified microsurgical techniques, aggressive anticoagulation, and anesthesia resulted in aneurysm patency rates and mortality rates comparable with those of the rabbit elastase model. Gross morphologic features of the created aneurysms are similar to those of most human intracranial aneurysms.

Acknowledgments

We thank the team of the Experimental Surgical Institute, University of Berne, for their excellent cooperation and extraordinary support. The authors are indebted to Professor Hanns Plenk, Jr, Department of Bone and Biomaterials Research at the Institute for Histology and Embryology, Medical University of Vienna, Austria, for his advice and review of the article. The authors thank Professor Heber Ferraz-Leite, Director of the European Workshop on Microsurgery and Cerebral Revascularization at the Medical University of Vienna, Austria, for his valuable microsurgical teaching.

References

1. Molyneux AJ, Kerr RS, Yu LM, et al. **International Subarachnoid Aneurysm Trial (ISAT) of neurosurgical clipping versus endovascular coiling in 2143 patients with ruptured intracranial aneurysms: a randomised comparison of effects on survival, dependency, seizures, rebleeding, subgroups, and aneurysm occlusion.** *Lancet* 2005;366:809–17
2. Mitchell P, Kerr R, Mendelow A, et al. **Could late rebleeding overturn the superiority of cranial aneurysm coil embolization over clip ligation seen in the International Subarachnoid Aneurysm Trial?** *J Neurosurg* 2008;108:437–42
3. Bavinzski G, Richling B, Binder BR, et al. **Histopathological findings in experimental aneurysms embolized with conventional and thrombogenic/antithrombolytic Guglielmi coils.** *Minim Invasive Neurosurg* 1999;42:167–74
4. Bocher-Schwarz HG, Ringel K, Bohl J, et al. **Histological findings in coil-packed experimental aneurysms 3 months after embolization.** *Neurosurgery* 2002;50:379–84, discussion 384–85
5. Sherif C, Plenk H Jr, Grossschmidt K, et al. **Computer-assisted quantification of occlusion and coil densities on angiographic and histological images of experimental aneurysms.** *Neurosurgery* 2006;58:559–66, discussion 559–66
6. Bouzeghrane F, Naggara O, Kallmes D, et al. **In vivo experimental intracranial aneurysm models: a systematic review.** *AJNR Am J Neuroradiol* 2010;31:418–23. Epub 2009 Oct 29
7. Massoud T, Guglielmi G, Ji C. **Experimental saccular aneurysms. 1. Review of surgically constructed models and their laboratory applications.** *Neuroradiology* 1994;36:537–46
8. Anidjar S, Salzmann J, Gentric D. **Elastase-induced experimental aneurysms in rats.** *Circulation* 1990;82:973–81
9. Wakhloo A, Schellhammer F, de Vries J. **Self-expanding and balloon-expandable stents in the treatment of carotid aneurysms: an experimental study in a canine model.** *AJNR Am J Neuroradiol* 1994;15:493–502
10. Dai D, Ding YH, Danielson MA, et al. **Histopathologic and immunohistochemical comparison of human, rabbit, and swine aneurysms embolized with platinum coils.** *AJNR Am J Neuroradiol* 2005;26:2560–68
11. Shin YS, Niimi Y, Yoshino Y, et al. **Creation of four experimental aneurysms with different hemodynamics in one dog.** *AJNR Am J Neuroradiol* 2005;26:1764–67
12. Abruzzo T, Shengelaia GG, Dawson RC 3rd, et al. **Histologic and morphologic comparison of experimental aneurysms with human intracranial aneurysms.** *AJNR Am J Neuroradiol* 1998;19:1309–14
13. Ding YH, Dai D, Lewis DA, et al. **Angiographic and histologic analysis of experimental aneurysms embolized with platinum coils, Matrix, and HydroCoil.** *AJNR Am J Neuroradiol* 2005;26:1757–63
14. Dai D, Ding Y, Danielson M, et al. **Endovascular treatment of experimental aneurysms with use of fibroblast transfected with replication-deficient adenovirus containing bone morphogenic protein-13 gene.** *AJNR Am J Neuroradiol* 2008;29:739–44. Epub 2008 Jan 9
15. Grunwald IQ, Romeike BF, Roth C, et al. **Anticoagulation regimes and their influence on the occlusion rate of aneurysms: an experimental study in rabbits.** *Neurosurgery* 2005;57:1048–55, discussion 48–55
16. Cawley CM, Dawson RC, Shengelaia G, et al. **Arterial saccular aneurysm model in the rabbit.** *AJNR Am J Neuroradiol* 1996;17:1761–66
17. Krings T, Moller-Hartmann W, Hans FJ, et al. **A refined method for creating saccular aneurysms in the rabbit.** *Neuroradiology* 2003;45:423–29
18. Cruise G, Shum J, Plenk H. **Hydrogel-coated and platinum coils for intracranial aneurysm embolization compared in three experimental models using computerized angiographic and histologic morphometry.** *J Mater Chem* 2007;17:3965–73
19. Yonekawa Y, Fandino J, Taub E. **Surgical therapy.** In: Fisher M, Borgousslavsky J, eds. *Current Review of Cerebrovascular Disease.* Philadelphia: Current Medicine; 2001:254
20. Sherif C, Marbacher S, Fandino J. **High-resolution three-dimensional 3T magnetic resonance angiography for the evaluation of experimental aneurysms in the rabbit.** *Neurol Res* 2009;31:869–72. Epub 2009 Feb 12
21. Bavinzski G, al-Schameri A, Killer M, et al. **Experimental bifurcation aneurysm: a model for in vivo evaluation of endovascular techniques.** *Minim Invasive Neurosurg* 1998;41:129–32
22. Plenk H, Shum J, Cruise G, et al. **Cartilage and bone neoformation in rabbit carotid bifurcation aneurysms after endovascular coil embolization.** *Eur Cell Mater* 2008;16:69–79
23. Sherif C, Bavinzski G, Dorfer C, et al. **Computerized assessment of angiographic occlusion rate and coil density in embolized human cerebral aneurysms.** *AJNR Am J Neuroradiol* 2009;30:1046–53
24. Spetzger U, Reul J, Weis J, et al. **Microsurgically produced bifurcation aneurysms in a rabbit model for endovascular coil embolization.** *J Neurosurg* 1996;85:488–95
25. Lall R, Eddleman C, Bendok B, et al. **Unruptured intracranial aneurysms and the assessment of rupture risk based on anatomical and morphologic factors: sifting through the sands of data.** *Neurosurg Focus* 2009;26:E2:1–5
26. Ohshima T, Miyachi S, Hattori K, et al. **Risk of aneurysm rupture: the importance of neck orifice positioning—assessment using computational flow simulation.** *Neurosurgery* 2008;62:767–75
27. Forrest MD, O'Reilly GV. **Production of experimental aneurysms at a surgically created arterial bifurcation.** *AJNR Am J Neuroradiol* 1989;10:400–02
28. Grunwald I, Romeike B, Roth C, et al. **Anticoagulation regimes and their influence on the occlusion rate of aneurysms: an experimental study in rabbits.** *Neurosurgery* 2005;57:1048–54
29. Lewis D, Ding Y, Dai D, et al. **Morbidity and mortality associated with creation of elastase-induced saccular aneurysms in a rabbit model.** *AJNR Am J Neuroradiol* 2009;30:91–94
30. Hoh BL, Rabinov JD, Pryor JC, et al. **A modified technique for using elastase to create saccular aneurysms in animals that histologically and hemodynamically resemble aneurysms in human.** *Acta Neurochir (Wien)* 2004;146:705–11
31. Cloft HJ, Altes TA, Marx WF, et al. **Endovascular creation of an in vivo bifurcation aneurysm model in rabbits.** *Radiology* 1999;213:223–28